J Mater Sci (2007) 42:8447–8453
DOI 10.1007/s10853-007-1783-7

Pulsed plasma nitriding of large components and coupons of chrome plated SS316LN stainless steel

Arup Dasgupta · P. Kuppusami · M. Vijayalakshmi · V. S. Raghunathan

Received: 27 November 2006 / Accepted: 16 April 2007 / Published online: 4 July 2007

Abstract Pulsed plasma nitriding of electroplated Cr on stainless steel substrates is reported. The properties of the chromium nitride coatings on small coupons synthesised simultaneously with large-scale components have been investigated. The effect of temperature and duration of the nitriding process on the coating properties are discussed. A gradual variation in the hardness profile from a peak hardness of about 950 HV at the surface to about 650 HV at 90 μm of case depth has been achieved. The chromium nitride coating was not brittle. The resistance of the coating to abrasive wear was higher than that for Cr. X-ray diffraction and energy dispersive X-ray analysis confirmed that the coating is composed of polycrystalline Cr_2N and Cr indicating that there was partial conversion of the electroplated Cr film to nitride.

Introduction

Hardfacing of stainless steel (SS) components is commonly used to improve the chemical and mechanical properties like surface hardness, resistance to wear, fatigue loading and corrosion [1]. For many applications, coatings need to withstand high operating temperatures. Amongst the various hardfacing materials, chromium nitride (CrN or Cr_2N) can attain hardness up to 2400 HV [2] and has excellent thermal stability up to ~1273 K. In fact, properties of chromium nitride coatings are superior to other coatings like TiN, with respect to lower coefficient of friction and better oxidation resistance [3]. Hard chromium nitride coatings are also preferable to stellite and colmonoy coatings in radioactive environments [4] owing to the significantly reduced induced radioactivity and superior mechanical properties.

Chromium nitride coatings are popularly synthesised either by direct Physical Vapour Deposition (PVD) [5–7] or Chemical Vapour Deposition (CVD) [8] techniques, or a two-step, indirect process of gas nitriding [9] or plasma nitriding [10–13] of a pre-deposited Cr layer. Of these, plasma nitriding is one of the most powerful surface modification techniques owing to several advantages [14], such as less warping and distortion, and superior resistance to wear, corrosion and fatigue. It also allows lower substrate-temperature treatment and avoids handling of hazardous and toxic chemicals and gases. Using a pulsed DC power-supply to generate the plasma instead of conventional DC has added advantages: (i) sputtering of the substrate by the positive ions is confined only to the 'ON' time of the duty cycle of the pulse, (ii) during the 'OFF' time of the pulse, there is no sputtering event, yet the species generated during the 'ON' time and responsible for nitriding remain active [15], (iii) rapid arcing resulting in the disruption of the nitriding process can be minimised, and (iv) it is possible to nitride narrow apertures by controlling the hollow cathode discharge [15–17], a phenomenon which gives rise to a special glow inside narrow apertures in the substrate. However, while hollow cathode discharge is advantageous in nitriding narrow apertures, it may give rise to extremely high temperatures locally resulting in local distortions. This phenomenon thus necessitates the measurement of distortion after nitriding.

A. Dasgupta (✉) · P. Kuppusami · M. Vijayalakshmi · V. S. Raghunathan
Physical Metallurgy Section, Materials Characterisation Group, Indira Gandhi Centre for Atomic Research, Kalpakkam 603 102, India
e-mail: arup@igcar.gov.in

It must be noted that although electroplated (EP)-Cr by itself offers high hardness (~900VHN), corrosion resistance and low coefficient of friction, these properties degrade severely under high temperature operating conditions. It has previously been shown by us [13] and other researchers [18] that the hardness of EP-Cr drops from an initial value of ~840VHN to about 360VHN at 773K. These results have demonstrated that EP-Cr is not suitable for high temperature applications. Hence, it is necessary to convert the EP-Cr layer into a more thermally stable compound such as a nitride of Cr. In this paper, the properties of the chromium nitride coatings developed by pulsed plasma nitriding of EP-Cr on SS substrates have been investigated.

Experimental

The substrates were Type 316LN SS cylindrical tubes about 970 mm long with an internal diameter of 80 mm and wall thickness of about 20 mm. It was necessary to hardface these components along their internal surface using chromium nitride coating. For this purpose, the work-pieces were machined as per requirement and their internal surfaces were electroplated with Cr up to 90 μm by M/s, MTAR Technologies, India. The external surface of the cylindrical component was mechanically masked using a tight-fit SS foil. For ease of experimentation, characterisation was carried out on representative coupons. These coupons (100 mm × 60 mm × 6 mm) were also made of the same material as the tubular component and also Cr-plated simultaneously with the long tubular components.

Figure 1a shows the schematic of the nitriding system. The cathode plate, cylindrical component and the small coupons were collectively negatively biased with respect to the chamber wall. An auxiliary electrode was powered with a constant –500 V DC with respect to the ground. The plasma thus generated at the auxiliary electrode (pilot plasma) was found to be useful for striking and also maintaining stable and uniform master plasma around the large tubular component. Since the plasma conditions are identical for the tube and coupons, the later is considered representative of the process. Sections were cut out from the nitrided coupons for evaluating properties of the coating.

The component and coupons were first degreased using acetone. The cathode plate was also scraped with a emery paper and wiped clean with acetone prior to each nitriding process. The system was evacuated by means of a roots and rotary pump (Edwards, UK). Commercial grade argon (Ar), nitrogen (N_2) and hydrogen (H_2) gases were used during the process. A 20 kW pulsed power supply (FCIPT, India) was used for generation of plasma. The pulse frequency used was 10 kHz while the duty cycle was set at 20%. The substrate was heated by the bombardment of the energetic ions in the plasma and hence, the substrate temperature could be varied by adjusting the voltage. The substrate temperature was measured by means of a K-type thermocouple attached directly to the cathode plate and provided with suitable isolation circuitry so as to avoid interference from the pulsed power. In addition, the chamber wall was heated to 673 K. By suitably selecting the power to the components and to the wall temperature, the temperature of the components could be controlled.

Figure 1b shows schematically the substrate temperature–time profile of the various stages involved. The system was initially evacuated to 1×10^{-2} mbar and then filled with Ar and H_2 gas mixture in the ratio of 5:1 up to a chamber pressure of 5 mbar and then evacuated to 0.5 mbar. Using the same ratio for the gas mixture and maintaining a chamber pressure of about 1.0 mbar, plasma was struck with a typical power density of ~300 mW/cm^2. This step involves $Ar^+ + H^+$ ion sputter-cleaning of the specimen surfaces. During this process, the native oxides on the surface of specimen were also removed by etching. It is noted that although Ar alone could have been used for sputter-cleaning, H_2 was used to obtain a smooth transition to the nitriding cycle. This etching cycle also resulted in an increase in substrate

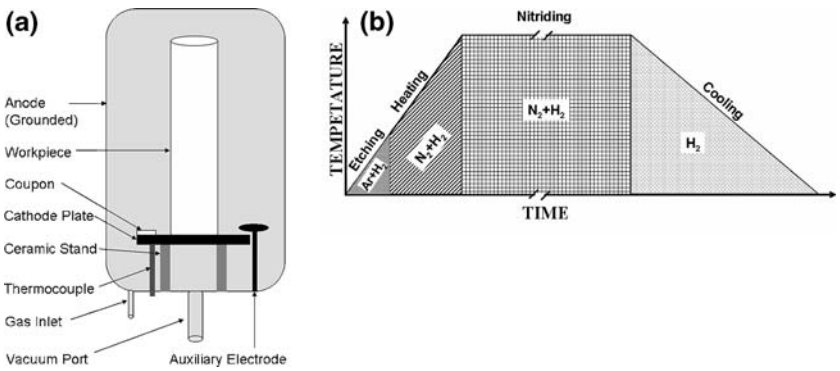

Fig. 1 (**a**) Schematic diagram of the specially designed plasma nitriding system used for large work-pieces. (**b**) Steps involved in the pulsed plasma nitriding process. The different gas mixtures used during the various process steps are indicated in the figure

temperature due to the impact of positive ions. This cycle was continued for 2 h. The wall heater was also switched on during this process and programmed to attain ~673 K at the rate of ~100 K/h. This was followed by the heating cycle in which Ar was replaced by N_2 gas without switching off the power supply. The ratio of flow of N_2 to H_2 gas and the chamber pressure were maintained at 3:1 and 3 mbar, respectively. The power density was also raised to a value between 360–450 mW/cm^2 depending on the final temperature that was desired. A constant substrate temperature was maintained by controlling the power density. The time duration for the nitriding processes were calculated from the time at which the desired substrate temperature was attainted to the time when the process was terminated. The nitriding process was terminated by switching off the power supply to the cathode as well as the wall heater. The system cooled down to room temperature by flowing H_2 gas at the rate of 100 sccm and maintaining a chamber pressure of about 5 mBar.

In this research work three samples with different nitriding temperature and nitriding durations were studied: (1) 773 K/50 h, (2) 843 K/9.5 h and (3) 913 K/45 h. Approximately 360 mW/cm^2 power was required for attaining a temperature of 773 K, and 450 mW/cm^2 was required for 913 K.

X-ray diffraction (XRD) studies of the coatings were performed using a Philips PW-1730 X-ray diffraction system fitted with a graphite crystal monochromator using CuKα radiation (λ = 1.541 Å) in θ–2θ geometry. The hardness of the coatings was measured with the help of a Leitz Miniload-2 Vickers micro-hardness testing machine using 100 and 500 g loads. The surface morphology of the coatings were examined with a Philips XL-30 ESEM (Environmental SEM) fitted with an energy dispersive X-ray (EDX) spectrometer for chemical analysis. The abrasive wear tests of the coatings were carried out in air at room temperature using a Calowear instrument (M/s CSEM Instruments SA, Switzerland). Calowear involves a rotating sphere technique, the details of which are described elsewhere [19].

Results and discussion

Visual inspection

The bright and lustrous Cr coating on the coupons as well as the inside the tubes bore greenish grey colour after nitriding, which is typical of the chromium nitride. The outside surface of the cylindrical component exhibited a steel finish since it has not been nitrided because of the mask. The results of various analyses of the coating are discussed in the following sections.

Structural and microchemical investigation

Figure 2 shows the X-ray diffraction pattern of the coating for two nitriding treatments examined, viz. 843 K/ 9.5 h (Fig. 2a) and 773 K/ 50 h (Fig. 2b). The diffraction patterns show reflections from various (hkl) planes of hexagonal β-Cr_2N [20] and body centred cubic (bcc) Cr [21]. However, no peaks corresponding to fcc CrN [22] are observed. The most intense peak for Cr (110) appearing at 2θ value of 44.2 degrees is much stronger than that for Cr_2N (111) appearing at 42.6 degrees. The ratio of the relative intensities of Cr (110) and β-Cr_2N (111) is higher when the nitriding condition was 843 K for 9.5 h than for 773 K/ 50 h. From these observations it may be inferred that: (a) β-Cr_2N is the only nitride of Cr to form; (b) there is a considerable amount of Cr that has not been converted to its nitride during the nitriding treatment; and (c) the degree of conversion of Cr to Cr_2N is higher at 773 K/ 50 h than at 843 K/ 9.5 h. The reason for obtaining superior nitridation at lower temperature is attributed to the diffusion kinetics that govern the nitriding process [13], whereby lower nitriding temperature can be compensated by longer duration. In our earlier report [13], it was argued that the initial formation of the nitride retards further diffusion of N thereby making the process rather slow. Thus, the period for nitriding was extended to 50 h at the lower temperature of 773 K. It is recognized that nitriding at lower temperatures is preferable as it can significantly reduce precipitation reactions in the work-pieces.

Figure 3 shows the energy dispersive X-ray spectra obtained from (a) chrome-plating and (b) the chromium nitride coating. Characteristic X-ray emission corresponding to Cr–K and Cr–L lines for both the samples can be

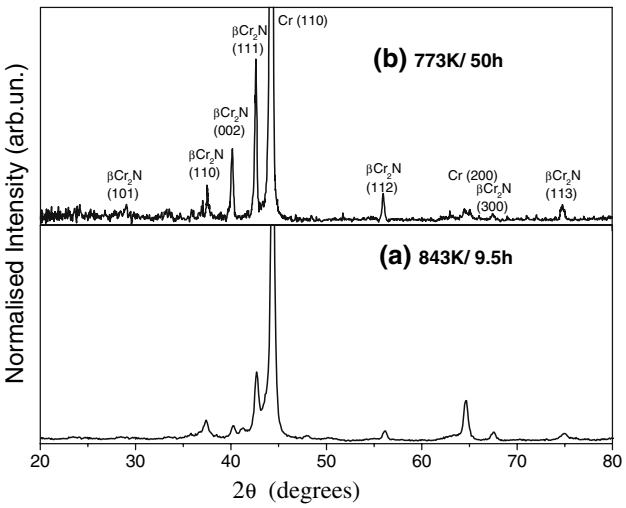

Fig. 2 XRD pattern of the samples nitrided at (**a**) 843 K for 9.5 h, and (**b**) 773 K for 50 h showing that the coating consists of a mixture of Cr and Cr_2N phases

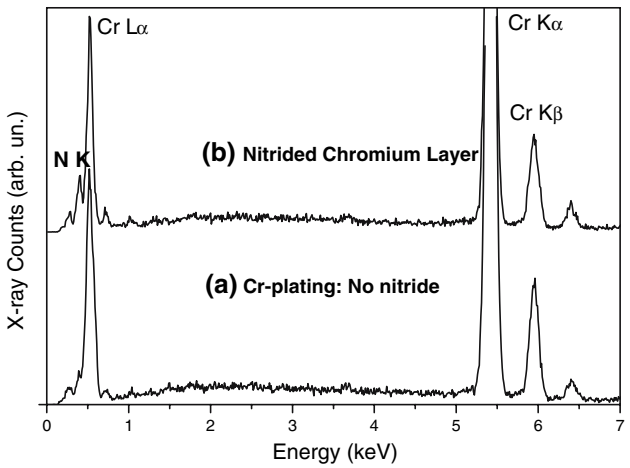

Fig. 3 EDS spectra obtained from (**a**) the chrome plated sample; and (**b**) the sample nitrided at 773 K for 50 h. The N–Kα peak is evident in (**b**)

seen in the figure. It is also observed that the chromium nitride sample exhibits a fairly strong N–K signal. This result supports the XRD analysis shown in Fig. 2, which confirms that electroplated Cr was partially converted to Cr_2N by pulsed plasma nitriding.

Investigation of hardness and abrasive wear properties

Figure 4 shows the cross-section profiles of Vicker's microhardness taken with 100 g load on the chromium nitride coatings formed at 773 K for 50 h. The hardness profiles for the 773 K/50 h chromium nitride coating were measured at two different locations, the average of which is shown by the solid curve in the figure. In addition, the

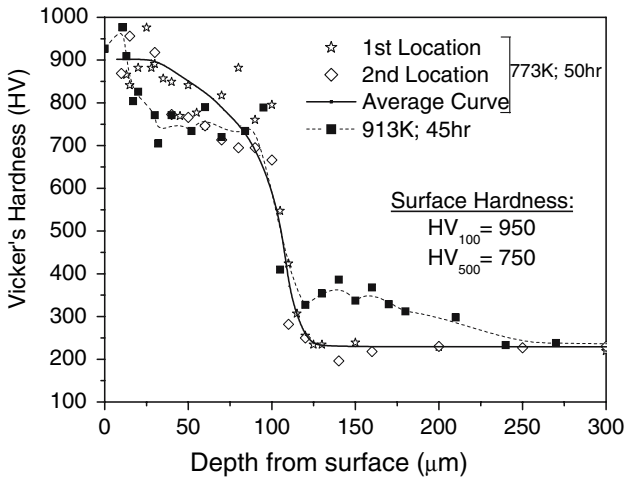

Fig. 4 Vicker's microhardness profile at two different locations for the sample nitrided at 773 K for 50 h. The average is shown by the solid curve. The hardness profile for the sample nitrided at 913 K for 45 h is also included for comparison

hardness profile obtained from a sample nitrided at 913 K for 45 h is shown by a dotted curve in the figure. For the solid curve, it is observed that the hardness value decreased gradually from a peak value 900 HV near the surface to about 400 HV at a depth of 110 μm and finally to ~200 HV at a depth of 125 μm. The change in hardness near the coating/ substrate (SS) interface is also gradual. It is observed that the average peak hardness for the 913K/ 45 h sample (dotted curve) is also about 900 HV. This value is much lower than hardness of Cr_2N (2400VHN). However, for nitriding temperatures of 773K and above, the hardness of EP-Cr is 360VHN or lower [13]. This indicates that the 90 μm EP-Cr film is only partially nitrided during this process, which is in agreement with the earlier observations. The smooth gradient of the hardness profiles is attributed to the diffusion-controlled mechanism of nitride formation [13]. A smooth hardness profile is necessary to avoid delamination of the coating from the substrate, in applications where the work-piece experiences large fluctuations in temperature. The delamination may result from a large difference in the thermal expansion coefficients (α) of Cr_2N and SS (α for Cr_2N is nearly 1/6th of that for SS). In fact, a multilayered Cr/CrN coatings have been reported to improve adhesion to steel substrates [23]. In addition to above, a marked difference in the gradient of the hardness profiles near the coating/ substrate interface, for the profiles corresponding to nitriding at 773 K and 913 K, are also observed. The hardness values near the interface are higher for the sample nitrided at 913 K/45 h than for 773 K/50 h. This can be understood in terms of possible inter-diffusion of Cr (from the EP-Cr layer) and Fe from the SS substrate at the interface at 913 K, the kinetics of which is much lower at 773 K.

The microhardness values measured using 100 g (HV_{100}) and 500 g (HV_{500}) loads on the surface of the chromium nitride coating synthesised under the standard conditions of 773 K and 50 h, are also listed in Fig. 4. It is observed that the HV_{100} is 950 but the HV_{500} is 750. The difference in the surface hardness values for different loads ($HV_{100} > HV_{500}$) may be attributed to: (1) the gradually decreasing hardness of the coating from the surface, and (2) the relatively soft SS316LN substrate (~200 HV). At higher loads such as 500 g, the indentation reaches deeper into the coating, where hardness is lower than that on the surface and thereby lowering the effective measured hardness. Secondly, as the indentation reaches closer to the soft SS substrate, the effective measured hardness will also be lower than the real value. It is well-known that, if the ratio of the indentation depth to coating thickness exceeds a certain critical value (normally ~0.07) [24, 25], the measured hardness is no longer characteristic of the coating alone but also includes a contribution from the substrate.

Figure 5 shows secondary electron (SE) images along the cross-section of chromium nitride coatings. Figure 5a–d

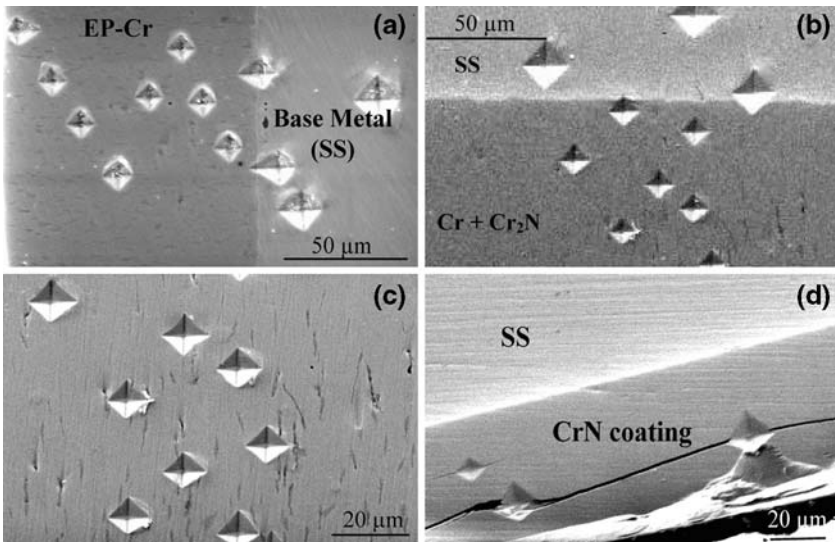

Fig. 5 SEM of the cross-section of coatings: (**a**) chrome plating, (**b**) Cr_2N coating prepared by pulsed plasma nitriding at 773 K for 50 h, (**c**) same as (**b**) at higher magnification showing that indentations do not result in crack formation, and (**d**) a polycrystalline CrN coating showing interconnected cracks due to indentation

show the images corresponding to EP-Cr on SS (base metal) substrate, chromium nitride coating processed by pulsed plasma nitriding of EP-Cr under standard conditions (773 K/50 h), the same chromium nitride coating at higher magnification and a chromium nitride coating deposited by PVD technique [26], respectively. Other than the rather featureless morphology of the coatings, these micrographs also show the indentation marks for 100 g load from Vicker's microhardness tester. From Fig. 5a it is seen that the diagonal lengths of the indentation are similar throughout the EP-Cr coating implying that the coating possesses a uniform hardness throughout its thickness. Figure 5b shows the variation of the indentation sizes in accordance with hardness profile shown in Fig. 4. Figure 5c shows that the chromium nitride coating possesses some unconnected microcracks, which owe their origin to the Cr-plating itself, and which are also evident from a careful inspection of Fig. 5a. However, the indentation does not lead to any crack formation indicating that the coating is not brittle. Figure 5d shows the micrograph of the cross-section of a polycrystalline CrN coating for comparison purposes. This coating is very hard (2000 HV) throughout its thickness (~20 μm), which decreased rapidly at the coating/SS interface. It can also be seen from the figure that indentation leads to formation of cracks, thereby demonstrating that such a hard coating is brittle.

Figure 6 shows the depth profiles of the abrasive wear rates (in mm^2/N) for the chromium nitride coating processed by pulsed plasma nitriding of EP-Cr under standard conditions (773 K/50 h) as compared to that of EP-Cr. It is observed that the abrasive wear rate for the Cr_2N coating is at least one order of magnitude lower than that for EP-Cr. The abrasive wear rate is lower near the surface of the Cr_2N coating, and it gradually increases with depth of the coating. Beyond the coating/ SS interface (i.e. ~90 μm, the thickness of the coating), the wear rate increases sharply indicating the beneficial effect of the coating on SS substrate. On the other hand, the wear rate is nearly constant for the EP-Cr coating near the coating/ SS interface, which increases in the SS substrate. Though the surface hardness of the EP-Cr and Cr_2N coating are almost same (~900 HV), Cr_2N is found to offer a superior abrasive wear property.

For large components, dimensional stability of large components is of utmost importance. Figure 7 shows the percentage change in dimensions of the tubular work-piece due to nitriding along the internal diameter (ID), which is actually chrome-nitrided, and also along the outer diameter (OD), which is masked during the nitriding process. The distance of this distortion measurement is calculated from one end of the 970 mm long tube. It is observed that the average distortion is less than ±0.15%, which is considered

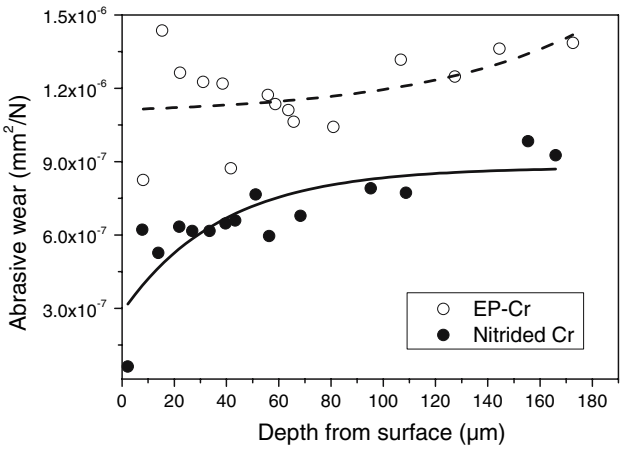

Fig. 6 Depth Profile of Abrasive Wear Rate (in air and at room temperature) of Cr_2N coating (standard conditions) as compared to that for Cr plating

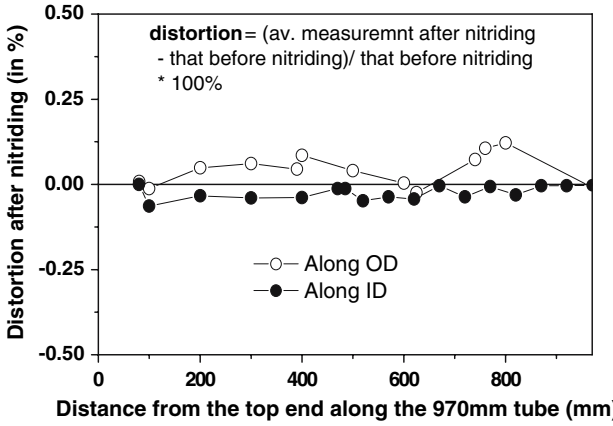

Fig. 7 Physical distortion of the work-piece due to nitriding at 773 K for 50 h

to be negligible. Hence the pulsed plasma nitriding process at 773 K for 50 h does not introduce any significant distortion in the work-pieces.

Understanding the nitriding process

In this process, electrons (e^-) emitted by the cathode due to the applied voltage are accelerated by the electric field. These energetic electrons collide with the gas molecules and ionise them. Although, formation of NH_x^+ (x = 0–2) from a N_2/H_2 gas mixture has been reported in the literature [27], the species responsible for nitriding are the N neutrals [28]. For the sake of simplicity, it may be assumed that N neutrals and ions are produced by cracking of N_2 gas. Accordingly, the various steps leading to the diffusion of nitrogen into the bulk of Cr layer are given below:

$$e^- + N_2 \rightarrow N + N + e^-$$
$$e^- + N \rightarrow N^+ + 2e^-$$
$$Energy_N^+ \rightarrow Energy_{heat} + Energy_{impulse}$$
$$Energy_{impulse} \rightarrow Cr(sputter)$$
$$Cr + N \rightarrow CrN\ (adsorbed);\ and$$
$$2Cr + N \rightarrow Cr_2N\ (adsorbed)$$
$$CrN + CrN \rightarrow Cr_2N + N\ (diffusing\ species)$$

Similar to all nitriding processes, diffusion of nitrogen into the base material depends on temperature. The immediate transfer of nitrogen from the plasma into the surface Cr layer could occur by direct ion inclusion. In addition, the atomic nitrogen (neutrals) in the plasma may also react directly with sputtered Cr forming CrN and Cr_2N. Since CrN has not been observed in the XRD results shown in Fig. 2, it is believed that they react in such a way so as to produce Cr_2N and N. This N could diffuse into the EP-Cr. Cr_2N, being a more stable molecule, is retained. The basis for this statement comes from the XRD data in Fig. 2 where it was observed that the coating contained significant amount of Cr_2N indicating that Cr_2N is more stable under the given plasma conditions. The stable Cr_2N layer that forms first on the surface of the coating may possibly retard the direct diffusion of N and hence slows down the diffusion kinetics resulting in long durations of nitriding. From this point of view, the process of indirect diffusion of N through reactions in metastable Cr–N and subsequent formation of Cr_2N appears to be the dominant mechanism for N transfer. The diffusion of this indirectly generated N is time-temperature dependent, the kinetics of which has been presented in our earlier study [13]. Therefore, if we accept that the diffusion of nitrogen leads to the formation of a hard Cr_2N phase in EP-Cr, the volume fraction of Cr_2N in EP-Cr is expected to follow an error function type of profile. This, in turn, will lead in a graded hardness profile as has been seen in Fig. 4. This mechanism of indirect diffusion of N through reactions in metastable chromium nitrides by virtue of plasma nitriding is a major advantage over other diffusive processes such as gas nitriding.

Conclusions

The development of chromium nitride coatings via a two-step process of Cr electroplating and plasma nitriding have been demonstrated. Hardfacing of large components and small coupons using the pulsed plasma nitriding of electroplated chromium has been performed. Nitriding of the electroplated Cr is partial. The measured surface hardness was about 950 HV, which was observed to decrease smoothly as a function of depth. Graded hardness in the coating is considered an important property for withstanding thermal shocks. The abrasive wear rate of the coating was nearly an order of magnitude superior to that for Cr. Furthermore, the lower temperature (773 K) nitriding process was found to impart negligible dimensional changes in the work-pieces.

Acknowledgment The authors gratefully acknowledge Dr. Baldev Raj, Director—IGCAR, Shri S.C Chetal, Director—REG, IGCAR and Dr. P.R. Vasudeva Rao, Director—MMG, IGCAR for their constant support and encouragement provided during the course of this research work. The authors also gratefully acknowledge the Central Workshop, IGCAR for building the masks for the work-piece and Quality Assurance Division, IGCAR for measuring the dimensional changes due to nitriding of the workpiece.

References

1. Bertrand G, Mahdjoub H, Meunier C (2000) 126:199
2. Kiuchi M, Funai M (1998) US patent no. 104352

3. Erturk E, Heuvel HJ, Dederichs HG (1989) Surf Coat Tech 39–40:435
4. Bhaduri AK, Indira R, Albert SK, Rao BPS, Jain SC, Asokkumar S (2004) J Nucl Mater 334:109
5. Aharonov RR, Coil BF, Fontana RP (1993) Surf Coat Tech 61:223
6. Navinsek B, Panjan P, Milosev I (1997) Surf Coat Tech 97:182
7. Münz WD, Hurkmans T, Keiren G, Trinh T (1993) J Vac Sci Technol A11:2583
8. Dasgupta A, Kuppusami P, Lawrence F, Raghunathan VS, Antony Premkumar P, Nagaraja KS (2004) Mater Sci Engg A374:362
9. Buijnsters JG, Shankar P, Sietsma J, Meulen JJ (2003) Mater Sci Engg A341:289
10. Menthe E, Rie KT (1999) Surf Coat Technol 112:1217
11. Wierzchon T, Ulbin-Pokorska I, Sikorski K (2000) Surf Coat Technol 130:274
12. Lunarska E, Nikiforow K, Wierzchon T, Ulbin-Pokorska I (2001) Surf Coat Technol 145:139
13. Kuppusami P, Dasgupta A, Raghunathan VS (2002) ISIJ Intl. 42:1457
14. Jones CK, Martin SW, Sturges DJ, Hudis M (1973) Heat Treatment '73. Metals Society, London, p 71
15. Kim YM, Han JG (2003) Surf Coat Technol 171:205
16. Gruen R, Guenther H (1991) Mater Sci Engg A140:435
17. Hugon R, Fabry N, Herrion G (1996) J Phys D Appl Phys 29:761
18. Alexander R (1996) Plat Surf Finish 7:9
19. Rutherford KL, Hutchings IM (1996) Surf Coat Technol 79:231
20. Powder diffraction file number 35-0803 from ICDD 1999
21. Powder diffraction file number 85-1336 from ICDD 1999
22. Powder diffraction file number 76-2494 from ICDD 1999
23. Lousa A, Romero J, Martinez E, Esteve J, Montata F, Carreras L (2001) Surf Coat Technol 146–147:268
24. Radic N, Stubicar M (1998) J Mat Sci 33:3401
25. Tuck JR, Korsunsky AM, Bull SJ, Elliott DM (2000) Surf Coat Tech 127:1
26. Dasgupta A, Vijayalakshmi M, Raghunathan VS, Raj B, Indira Gandhi Centre for Atomic Research, Internal Report
27. Hudis M (1973) J Appl Phys 44:1489
28. Tibbetts GG (1974) J Appl Phys 45:5072